Journal of Molecular Structure 1246 (2021) 131170

Contents lists available at ScienceDirect

Journal of Molecular Structure

journal homepage: www.elsevier.com/locate/molstr

Coumarin-Benzothiazole Based Azo Dyes: Synthesis, Characterization, Computational, Photophysical and Biological Studies

Manjunatha B[a], Yadav D. Bodke[a,*], Nagaraja O[b], Lohith T. N[c], Nagaraju G[d], Sridhar MA[c]

[a] Department of P.G. Studies and Research in Chemistry, Jnana Sahyadri, Kuvempu University, Shankaraghatta-577451, Shivamogga, Karnataka, India
[b] Department of P.G. Studies and Research in Industrial Chemistry, Jnana Sahyadri, Kuvempu University, Shankaraghatta-577451, Shivamogga, Karnataka, India
[c] Department of P.G. Studies and Research in Physics, Manasagangotri, University of Mysore, Mysuru-570 006, India
[d] Energy Materials Research Laboratory, Department of Chemistry, Siddaganga Institute of Technology, Tumakuru-572103, India

ARTICLE INFO

Article history:
Received 27 April 2021
Revised 20 July 2021
Accepted 21 July 2021
Available online 26 July 2021

Keywords:
Azo dyes
Computational studies
Photophysical properties
Antimycobacterial activity
In silico Molecular docking

ABSTRACT

In this paper, we have reported the synthesis of some coumarin-benzothiazole based azo dyes ($\mathbf{C_1}$-$\mathbf{C_5}$). The structure of the synthesised dyes was precisely established from their IR, NMR and HRMS spectra. The synthesised dyes were photophysically characterized by UV-Vis and Photoluminescence studies. Through the computational study, the optimized molecular geometry, and reactive parameters were investigated to get a better insight into the molecular properties. Molecular electrostatic potential (MEP) and Reduced density gradient (RDG) were also studied for all the compounds. Diffuse reflectance study was carried out to determine the energy gap (Eg) of the synthesised dyes. Additionally, the synthesized compounds were screened for their pharmacological property against *Mycobacterium tuberculosis* (H37 RV strain). The *in silico* molecular docking study was also performed with enoyl-ACP reductase.

1. Introduction

In present days coumarins have vital interest due to their dominance in natural product chemistry, and have a wide range of pharmacological properties and excellent optical properties [1-5]. Coumarin and its derivatives have been reported to use in optoelectronics (OLEDs), solar cells, lasers, nonlinear optics (NLO) and dye industries [6-9] due to their favourable characteristics such as solid state emission, large stokes shift, high emission yield, significant photo-physical properties and thermal stability. Coumarin derivatives have been also reported to possess very good efficacy in anti-inflammatory [10], antituberculosis [11], anti-HIV [12], antifungal [13], anti-tubulin [14], anti-coagulant [15] and antioxidant activity [16].

Azo dyes are colored organic compounds and are reported to have excellent absorption, emission, molar absorption coefficient, solvatochromic behaviour and undergo photochemical and thermal isomerization [17-20]. The recent few reports evidenced that 4-hydroxy coumarins having azo chromophore substitution at 3rd position exhibited very good optical properties, thermal stability and biological efficacy due to the increase in conjugation system between coumarin and other heterocycles through azo chromophore or other functionalities [21-23].

Benzothiazole pharmacophore is known to exhibit anticonvulsant [24], anti-inflammatory [25], antitumor [26] and antimicrobial activity [27]. This core also acts as fluorophore and chromophore which enhances the photophysical properties of the synthesized dyes [28,29]. Tuberculosis (TB) is the ninth cause of global death, more than any other infectious diseases and caused by *Mycobacterium tuberculosis* [30]. The serious problem associated with the treatment of TB is the emergence of resistance and the cause of resistance is the genetic mutation [31]. Present antituberculosis agents are inefficient to bring down the ever increasing incidence of TB worldwide [32-34] and there are very less number of potential chemical entities in the TB drug pipeline. To overcome the high rates of abrasion, many more need to be discovered.

Literature findings revealed that some of the coumarin conjugates containing 4-hydroxy coumarin along with other heterocycles such as benzothiazole, antipyrene, sulfametazine etc exhibited promising antimicrobial, anticancer and antitberculosis activity [35-38]. Further they are known to possess good photophysical properties [39-41].

From the literature survey, it was found that the density functional theory (DFT) was used to explore molecular properties like structural properties, physicochemical properties, etc [42,43]. A set of global and local descriptors calculated from DFT calculations

* Corresponding author.
E-mail address: ydbodke@gmail.com (Y.D. Bodke).

https://doi.org/10.1016/j.molstruc.2021.131170
0022-2860/

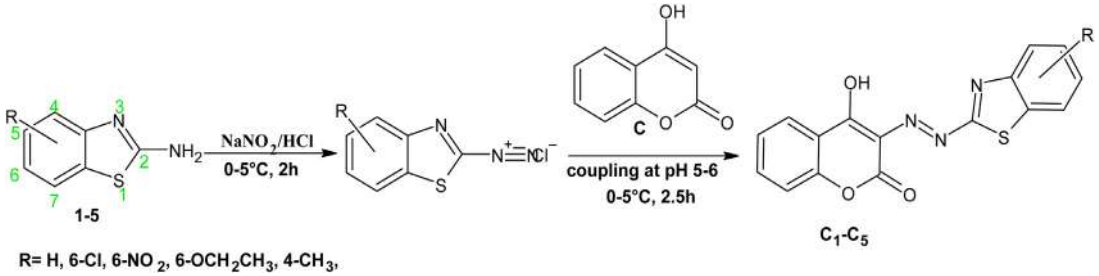

Scheme 1. Schematic route for the synthesis of coumarin azo dyes (C_1-C_5)

contributes to measure the reactivity and nature of the molecules [44,45].

These research findings encourage us to couple benzothiazole ring and 4-hydroxy coumarin through the azo group and to examine their photophysical properties, computational study, antimycobacterial efficacy and *in silico* molecular docking study.

2. Experimental

2.1. Materials and methods

All the chemicals and solvents used for the synthesis of coumarin dyes are of analytical grade (AR) and purchased from Sigma-Aldrich and Spectrochem. Melting point was recorded in a capillary tube on an electrothermal apparatus and are uncorrected. The FT-IR spectra were recorded on Bruker Alpha-T Attenuated Total Reflection Fourier Transform Infrared (ATR-FTIR) spectrometer between the frequency range 4000-400 cm^{-1}. The electronic absorption spectra were recorded on UV-1800 Shimadzu spectrophotometer in the range of 200–800 nm and Photoluminescence spectra were recorded using Agilent Technologies-Cary Eclipse Fluorescence Spectrophotometer. The ^{1}H NMR and ^{13}C NMR spectra were recorded with the aid of Bruker spectrometer of 400 MHz and 100 MHz respectively; chemical shifts (δ) were recorded in parts per million (ppm) using tetramethylsilane (TMS) as an internal reference. The HR-MS spectra were recorded on Waters Xevo G2-XS QTof mass spectrometer.

2.2. Computational studies

All computational calculations have been performed on a computer using the Gaussian 09 software [46] and B3LYP was used for the DFT calculations with a 6-31G (d,p) basis set [47,48]. Output files of the Gaussian software were visualized by using *Gaussview 05* [49]. MEP and RDG calculations were done using *Multiwfn 3.7* [50] and visualized using *Visual Molecular Dynamics* (VMD) software [51].

2.3. General procedure for the synthesis of coumarin-benzothiazole azo dyes (C_1-C_5)

Substituted 2-amino benzothiazole (1-5) was dissolved in 10 mL of HCl and cooled to 0-5°C. To this, ice-cold solution of $NaNO_2$ (5 mL) was added dropwise and stirred for 2 h at 0-5°C. After completion of diazotization, the obtained diazonium salt solution was added dropwise to the ice-cold aqueous KOH solution of 4-hydroxy coumarin (C). The reaction mixture was stirred for another 2 h at the same temperature. The pH of the reaction was maintained at 5-6 by using 10% sodium bicarbonate solution during stirring and the progress of the reaction was monitored by TLC. Further, the obtained coloured precipitate of the respective azo dyes (C_1-C_5) was separated by filtration, washed with distilled water followed by dil HCl, dried and recrystallized from ethanol. The schematic representation for the synthesis of azo dyes was displayed in Scheme 1.

2.3.1. 3-(1,3-Benzothiazol-2-yldiazenyl)-4-hydroxy-2H-chromen-2-one (C_1)

Orange powder, Yield 85%, purity (%): 94.62, m p: 224-226°C. IR(cm^{-1}): 3446 (-OH), 3049 (Ar-CH), 1749 (C=O), 1615 (C=N), 1515 (N=N), 1482(Ar-C=C). ^{1}H NMR (DMSO-d_6, δ ppm): 7.35 (m, 3H, Ar-H), 7.47 (t, J=7.2 Hz, 1H, Ar-H), 7.77 (m, 1H, Ar-H), 7.81 (d, 7.6 Hz, 1H, Ar-H), 7.99 (m, 1H, Ar-H), 8.04 (d, 8Hz, 1H, Ar-H). ^{13}C NMR (DMSO-d_6, δ ppm): 165.22, 157.57, 154.54, 151.01, 137.38, 132.26, 127.34, 127.02, 125.57, 125.26, 123.05, 122.24, 121.07, 117.86. HR-MS: *m/z* (%) = 324.1071 $[M+H]^+$. Anal. Calcd $C_{16}H_9N_3O_3S$: C, 59.44%; H, 2.81%; N, 13.00% Found: C, 59.24%; H, 2.68%; N, 12.91%.

2.3.2. 3-[(6-Chloro-1,3-benzothiazol-2-yl)diazenyl]-4-hydroxy-2H-chromen-2-one (C_2)

Orange powder, yield 89%, purity (%): 96.83, m p: 212-214°C. IR(cm^{-1}): 3417 (-OH), 3083 (Ar-CH), 1754 (C=O), 1615 (C=N), 1517 (N=N), 1489 (Ar-C=C), 760 (C-Cl). ^{1}H NMR (DMSO-d_6, δ ppm): 7.35 (m, 3H, Ar-H), 7.49 (m, 1H, Ar-H), 7.76 (m, 2H, Ar-H), 7.9 (d, 7.6 Hz, 1H, Ar-H), 8.2 (d, 7.2 Hz, 1H, Ar-H).^{13}C NMR (DMSO-d_6, δ ppm): 171.79, 159.56, 157.52, 154.55, 150.13, 144.05, 137.42, 133.97, 129.71, 127.66, 127.35, 125.28, 123.46, 122.75, 121.06, 117.87, 108.64. HR-MS: *m/z* (%) = 358.0699 $[M+H]^+$. Anal. Calcd $C_{16}H_8ClN_3O_3S$: C, 53.21%; H, 2.25%; N, 11.74% Found: C, 52.94%; H, 2.18%; N, 11.56%.

2.3.3. 4-Hydroxy-3-[(6-nitro-1,3-benzothiazol-2-yl)diazenyl]-2H-chromen-2-one (C_3)

Yellow powder, yield 75%, purity (%): 95.89, m p: 198-200°C. IR(cm^{-1}): 3424 (-OH), 3097 (Ar-CH), 1747 (C=O), 1616 (C=N), 1521 (N=N), 1466 (Ar-C=C). ^{1}H NMR (DMSO-d_6, δ ppm): 7.28 (m, 3H, Ar-H), 7.67 (t, 7.6 Hz, 1H, Ar-H), 7.94 (m, 2H, Ar-H), 8.24 (d, 8.4 Hz, 1H, Ar-H), 8.98 (s, 1H, Ar-H). HR-MS: *m/z* (%) = 369.0903 $[M+H]^+$. Anal. Calcd $C_{16}H_8N_4O_5S$: C, 52.17%; H, 2.19%; N, 15.21% Found: C, 52.11%; H, 2.01%; N, 15.18%.

2.3.4. 3-[(6-Ethoxy-1,3-benzothiazol-2-yl)diazenyl]-4-hydroxy-2H-chromen-2-one (C_4)

Red powder, yield 79%, purity (%): 96.5, m p: 246-248°C. IR(cm^{-1}): 3419 (-OH), 2982 (Ar-CH), 1749 (C=O), 1607 (C=N), 1555 (N=N), 1487 (Ar-C=C). ^{1}H NMR (DMSO-d_6, δ ppm): 1.33 (t, 3H, CH_3), 3.98 (q, 2H, -OCH_2-), 6.99 (s, 1H, Ar-H), 7.04 (d, 6.4 Hz, 1H, Ar-H), 7.32 (m, 2H, Ar-H), 7.62 (m, 3H, Ar-H), 7.98 (d, 6.4 Hz, 1H, Ar-H). HR-MS: *m/z* (%) = 368.1315 $[M+H]^+$. Anal. Calcd $C_{18}H_{13}N_3O_4S$: C, 58.85%; H, 3.57%; N, 11.44% Found: C, 58.81; H, 3.41; N, 11.36%

2.3.5. 4-Hydroxy-3-[(4-methyl-1,3-benzothiazol-2-yl)diazenyl]-2H-chromen-2-one
(C_5)

Red orange powder, yield 89%, purity (%): 97.2, m p: 231-234°C. IR(cm^{-1}): 3444 (-OH), 2924 (Ar-CH), 1750 (C=O), 1613 (C=N), 1522 (N=N), 1489 (Ar-C=C).^{1}H NMR (DMSO-d_6, δ ppm): 2.59 (s, 1H, CH_3), 7.28-7.40 (m, 4H, Ar-H), 7.76 (t, 8 Hz, 1H, Ar-H), 7.85 (d, 7.2 Hz, 1H, Ar-H), 8.00 (d, 7.6Hz, 1H, Ar-H). HR-MS: *m/z* (%) = 338.1166 $[M+H]^+$. Anal. Calcd $C_{17}H_{11}N_3O_3S$: C, 60.52%; H, 3.29%; N, 12.46% Found: C, 60.34%; H, 3.18%; N, 12.39%.

2.4. Pharmacology

2.4.1. Antimycobacterial activity

The antimycobacterial activity was carried out at Dept of Microbiology, Maratha Mandal's NGH Institute of Dental Sciences & Research Centre, Belgaum, Karnataka. The antimycobacterial activity of synthesised compounds was screened against *Mycobacterium tuberculosis* (H37 RV strain) using microplate Alamar Blue assay (MABA) [52]. According to this method, 200 μL of sterile deionized water was added to all outer perimeter wells of sterile 96 wells plate to minimize evaporation of medium in the test wells during incubation. Then, 100 μL of the Middlebrook 7H9 broth was added to 96 wells plate and serial dilution of compounds were made directly on a plate. The final dye concentrations were between 100 to 0.2 μg/mL. Plates were covered with parafilm and incubated at 37°C for five days. Then, 25μl of freshly prepared 1:1 mixture of Almar Blue reagent and 10% tween 80 was added to the plate and incubated for 24 h. The blue color in the well was authenticated as no bacterial growth, and the pink color was scored as growth. The results of the study were interpreted in terms of minimum inhibitory concentration (MIC) using streptomycin as a standard.

2.4.2. in silico *Molecular docking studies*

The structure of synthesized molecules and standard drug were drawn using the Chem Bio Draw tool (Chem Bio Office Ultra 14.0 suite) and the energy minimization was performed using the Dundee prodrg server [53]. The ligand was further converted into PDBQT with the help of 'MGL tools' graphical interface program [54]. The protein data bank (PDB: 2 × 22) coordinate file with the name PT70 was used as a receptor molecule in anti-mycobacterial activity [55]. 'MGL tools', was used to adjust the gridbox to run docking simulations. Autodock Vina was used to explore the best docked conformation of compounds with protein and also the binding affinity. LigPlot+ and PyMol were used to infer the pictorial depiction of the interaction between the ligands and the target protein.

3. Results and discussion

3.1. DFT Studies

3.1.1. Frontier molecular orbitals (FMOs)

The structure of the compounds C_1-C_5 was optimized through B3LYP/6-31G(d,p) method and have been shown in supplementary material (Fig. S1-S5). The frontier molecular orbitals (HOMO and LUMO) determines the way in which the molecule interacts with the other molecules [56]. HOMO-LUMO energy gap helps to depict the kinetic stability and chemical reactivity of the molecule [57,58]. A molecule with a small gap is more polarized and is said to be a soft molecule; the larger the gap, the harder is the molecule. The FMOs of these derivatives were determined using the B3LYP/6-31G(d,p) method are plotted in Fig. 1.

The global reactivity parameters such as Electronegativity (χ), chemical potential (μ), global hardness (η), global softness (S) and electrophilicity index (ω) are calculated using the energies of frontier molecular orbitals as

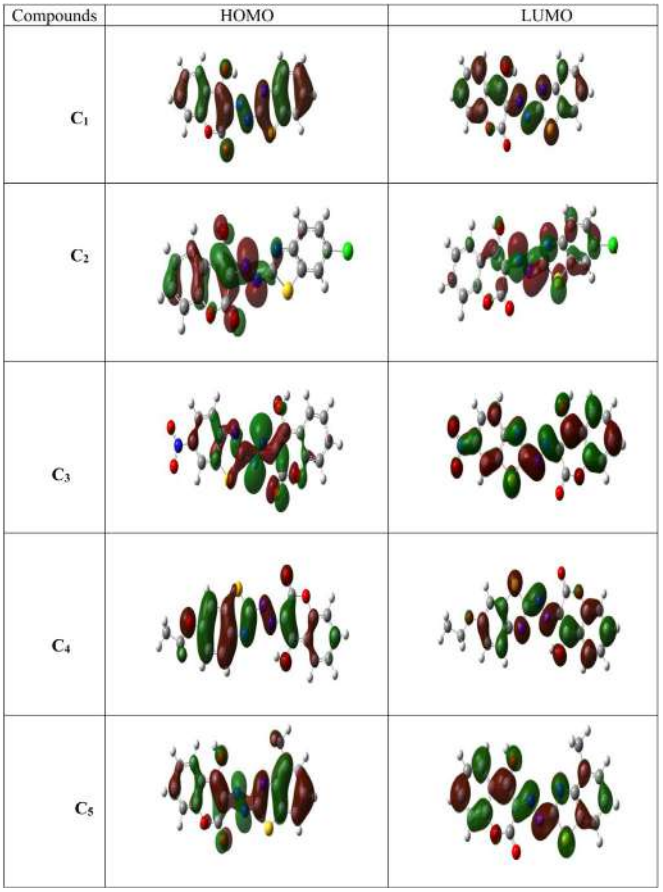

Fig. 1. The structure of the HOMO and LUMO of the compounds (C_1-C_5) generated from B3LYP method using 6-31G(d,p) basis set

$$\chi = -1/2(E_{HOMO} + E_{LUMO}),$$

$$\mu = -\chi = 1/2(E_{HOMO} + E_{LUMO}),$$

$$\eta = 1/2(E_{HOMO} - E_{LUMO}),$$

$$S = 1/2\eta$$

$$\omega = \mu^2/2\eta$$

To analyse the chemical behaviour of synthesized coumarin dyes (C_1-C_5), we evaluated their global and local reactivity parameters. The values of μ, χ, S, and ω were calculated and the results are listed in Table 1.

From the results, it was found that the chemical hardness value of the compound C_4 is lesser compare to other synthesised compounds. Thus, compound C_4 is found to be more reactive. Further, noted that compound C_3 is having a higher electronegativity value among the synthesised compounds, hence it is the best electron acceptor among the synthesised dyes (C_1-C_5).

The FMO gap helps to characterize molecular electrical transport properties, the chemical reactivity and kinetic stability of the molecule [59]. A molecule with a small FMO gap is generally associated with a high chemical reactivity and low kinetic stability. Larger the HOMO-LUMO energy gap, the harder the molecule.

Table 1
Global reactive parameters calculated for compounds C_1-C_5

Parameters	C_1	C_2	C_3	C_4	C_5
E_{HOMO} (eV)	-6.110	-6.287	-6.355	-5.674	-5.879
E_{LUMO} (eV)	-2.940	-3.240	-3.233	-2.818	-2.757
Energy gap (Δ) (eV)	3.170	3.047	3.123	2.856	3.122
Ionization energy (I) (eV)	6.110	6.287	6.355	5.674	5.879
Electron affinity (A) (eV)	2.940	3.240	3.233	2.818	2.757
Electronegativity (χ) (eV)	4.525	4.763	4.794	4.246	4.318
Chemical potential (μ) (eV)	-4.525	-4.763	-4.794	-4.246	-4.318
Global hardness (η) (eV)	1.585	1.523	1.561	1.428	1.561
Global softness (S) (eV^{-1})	0.631	0.656	0.640	0.700	0.641
Electrophilicity index (ω) (eV)	6.460	7.447	7.359	6.312	5.973

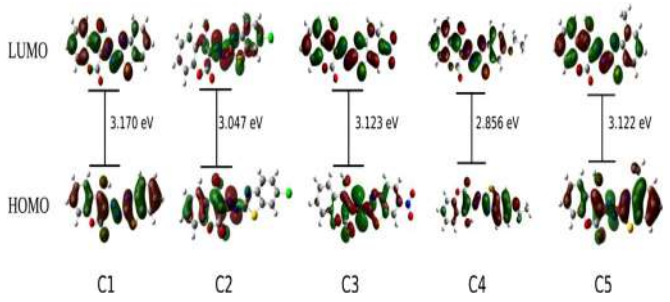

Fig. 2. Theoretically calculated HOMO-LUMO gap of compounds (C_1-C_5)

HOMO-LUMO energy gap of the compounds (C_1-C_5) have been displayed in Fig. 2. The HOMO-LUMO energy gap of compounds C_1, C_2, C_3, and C_5 was slightly larger, signifying higher excitation energy in comparison to C_4, it may be because of electron donating tendency of –OEt group present at the 6th position of benzothiazole. Hence compounds C_1, C_2, C_3 and C_5 are harder in comparison to compound C_4.

3.1.2. Molecular electrostatic potential Map (MEP)

Electrostatic surface potential (ESP) maps, also known as electrostatic potential energy maps, or molecular electrical potential surfaces, illustrate the three-dimensional charge distributions over the molecules [60]. MEP provides a visual method to understand the reactive polarity of the molecule. The negative electrostatic potential corresponds to an attraction of the proton by the electron density of the molecules. The positive electrostatic potential corresponds to the repulsion of the proton by the atomic nuclei in regions where low electron density exists. The electrostatic potential surface was calculated by DFT/B3LYP at 6-31G(d,p) basis set and plotted in Fig. 3. The different values of the electrostatic potential are represented by different colors; the most negative electrostatic potential as red, the regions of the most positive electrostatic potential as blue and the region of zero potential as green. From Fig. 3, we observed that, the more negative electrostatic potential is found around the carbonyl oxygen and azo group, the more positive electrostatic potential is observed around the –OH group attached to the coumarin ring at the 4th position for all the compounds. The hydrogen atoms attached to the heterocyclic rings have zero potential. The overall volume of the surface, minimum and maximum electrostatic potential surface was listed in Table 2.

3.1.3. Reduced density gradient analysis

Reduced density gradient (RDG) analysis is used to explore weak interactions in real space based on the electron density and its derivatives [61]. The RDG is a dimensionless quantity obtained from electron density (ρ) and calculated as

$$RDG(r) = \frac{\Delta p(r)}{2(3\pi^2)^{(1/3)} p(r)4/2}$$

Table 2
Volume of the surfaces and electrostatic potential of the compounds (C_1-C_5).

Compounds	Volume of the surface (Å^3)	Electrostatic Potential (kcal/mol)	
		Minimum	Maximum
C_1	347.449	-51.809	70.204
C_2	368.736	-48.378	71.978
C_3	376.347	-42.412	75.482
C_4	403.015	-47.975	49.724
C_5	369.889	-50.245	70.151

The weak interactions are shown in the region with low electron density and low RDG. The interaction type can be found out with the electron density ρ multiplied by the sign of λ_2 with RDG. The scattered reduced density gradient for the compounds C_1-C_5 have been shown in Fig. 4.

The RDG versus sign of $(\lambda_2)\rho$ peaks provides information about the nature of the interaction. The RDG=0.2 lines are evaluated in these molecules and crossed the repulsive spikes. Large negative values of sign $(\lambda_2)\rho$ are indicative of stronger attractive interactions, while positive ones are indicative of strong repulsion interactions. Values near zero indicate very weak Van der Waals interactions. The colour from blue to red means stronger attraction to repulsion respectively. The green colour circles can be identified as Vander Waals interaction region, which means that electron density in these regions is low. Fig. 4 displayed that the molecules C_1-C_5 have strong repulsion or steric effect in the ring, and the Vander Waals interactions were observed between the carbonyl oxygen and the nitrogen atom of the azo group and between the nitrogen atom of the benzothiazole and azo group.

3.2. UV-Vis spectra

The electronic spectra of the coumarin azo dyes (C_1-C_5) were recorded in five different solvents (n-Hexane, Toluene, Ethanol, DMF, and DMSO) in the range 200-800 nm (10^{-4} M solution) to study the solvent effect on electronic spectra of the dyes C_1-C_5. The electronic spectra of individual compounds (C_1-C_5) recorded in different solvents were given in Fig. 5-9. The values of the electronic spectral data were tabulated in Table 3. The electronic spectral results displayed that the azo dyes exhibit characteristic absorption bands in the range of 406-488nm, that probably due to $\pi \rightarrow \pi^*$ and/or $n \rightarrow \pi^*$ transition.

All the synthesized dyes (C_1-C_5) showed a solvatochromic behaviour in studied solvents, and found that absorption remarkably dependent on the polarity of solvents. As we move from nonpolar (Hexane) to polar (DMSO), red shift is observed. This can be attributed to the interaction of lone pair of electrons on the nitrogen atom of the azo group as well as the pi-electrons of the aromatic system with solvents. This demonstrates the remarkable positive solvatochromic behaviour of the synthesised dyes.

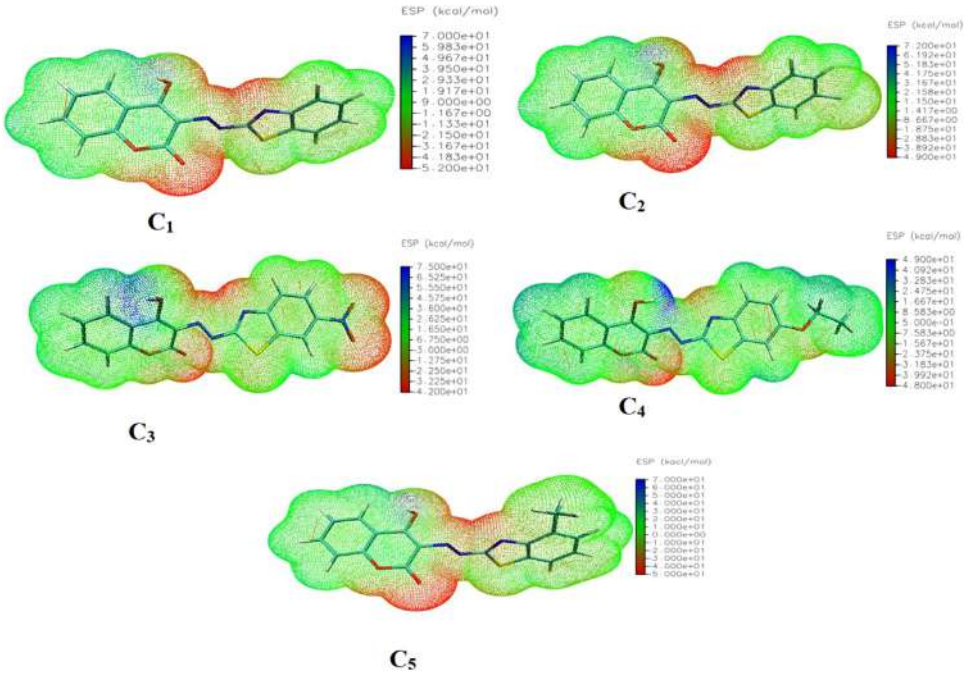

Fig. 3. Molecular electrostatic potential of the synthesized dyes (C_1-C_5)

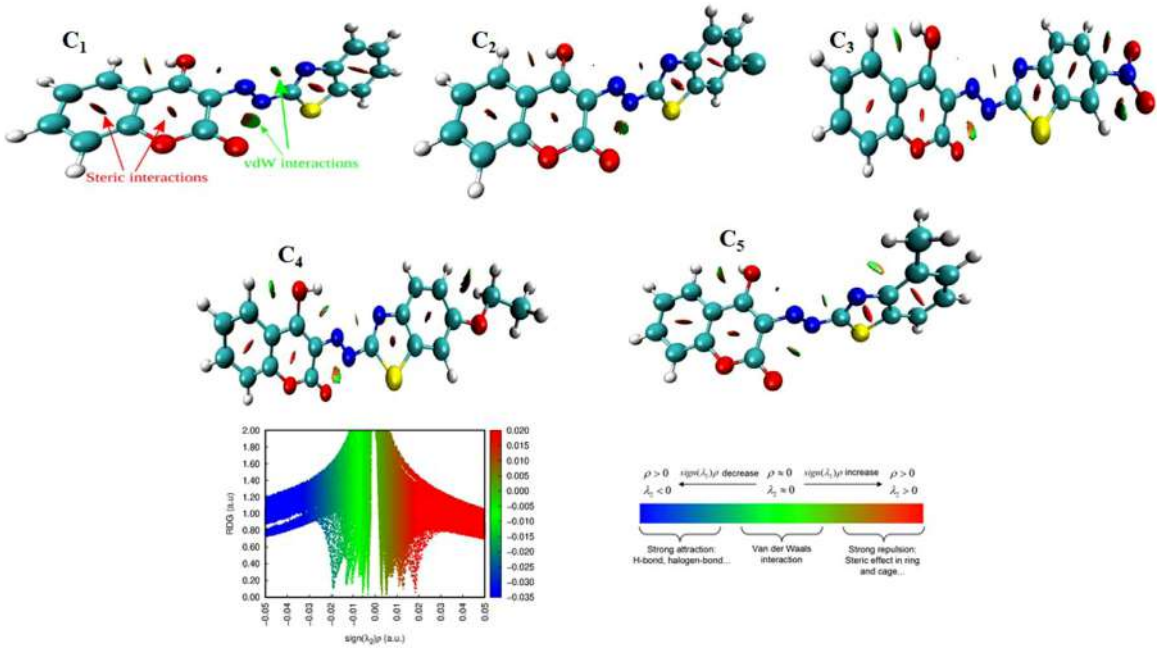

Fig. 4. Plots of the RDG versus the electron density multiplied by the sign of the second Hessian Eigen value (λ_2) and the colored surfaces of the compound (C_1-C_5) according to values of sign λ_2

The comparative graph of λ_{max} of synthesised compounds (C_1-C_5) in studied solvents was given in Fig. 10. From the Fig. 10, we observed that the presence of electron-donating (–OEt) substituent at 6th position in C_4 exhibited a red shift compared to unsubstituted dye C_1. Compound C_3 containing -NO_2 substituent at 6th position caused a red shift compared to C_1. Compounds C_2 and C_4 having -Cl and -Me substituent at 6th and 4th position respectively, caused a blue shift compared to unsubstituted dye C_1.

3.3. Fluorescence spectral data

The emission study of the coumarin dyes (C_1-C_5) has been explored in various aprotic and protic solvents between the range from 480 to 700 nm. The emission spectra of all the dyes (C_1-C_5) were recorded in the concentration of 10^{-4} M solution at room temperature. The emission profile of the synthesised dyes was also appended in Table 3 and the emission spectra were shown in Fig. 11-15.

The comparative graph of $\lambda_{emission}$ of synthesised compounds (C_1-C_5) in studied solvents was displayed in Fig. 16. From Fig. 16, it was found that compounds C_4 and C_5 showed redshift compared to unsubstituted dye C_1, this may be attributed to the presence of electron-releasing groups like –OEt and –Me at a 6th and 4thposition of the benzothiazole nucleus. Electron withdrawing groups like –Cl, -NO_2 causes the emission shift towards blue wavelength in compound C_2 and C_3 respectively.

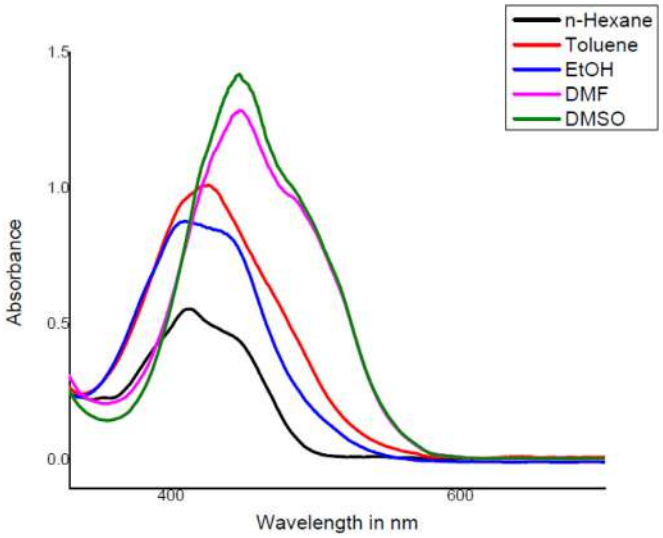

Fig. 5. Absorption spectra of dye C_1 in different solvents (10^{-4} M)

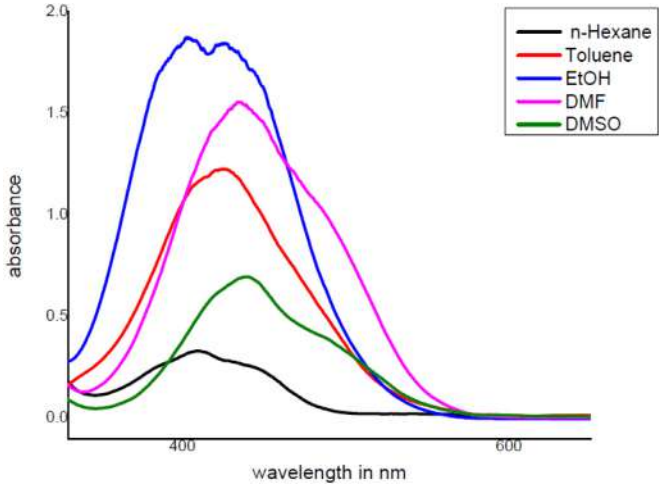

Fig. 6. Absorption spectra of dye C_2 in different solvents (10^{-4} M)

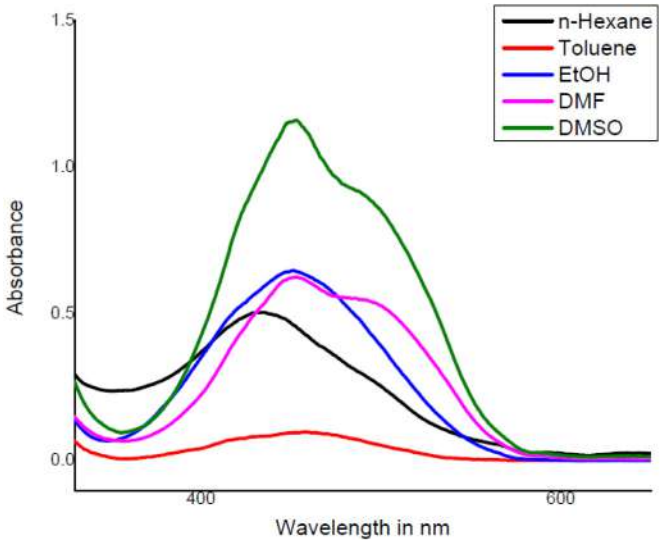

Fig. 7. Absorption spectra of dye C_3 in different solvents (10^{-4} M)

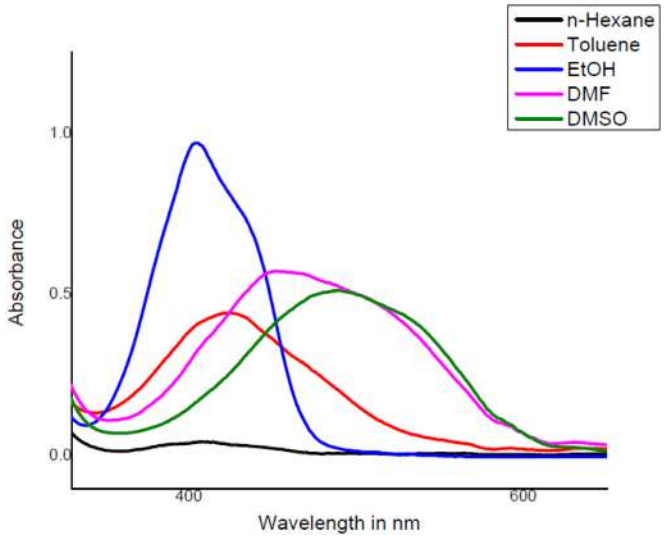

Fig. 8. Absorption spectra of dye C_4 in different solvents (10^{-4} M)

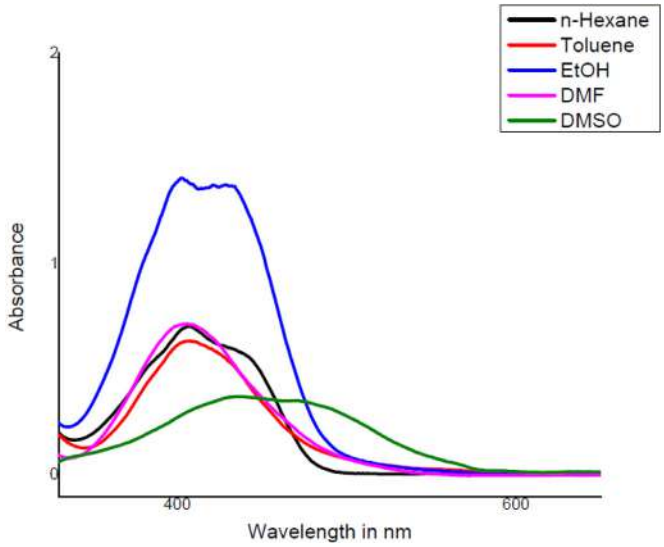

Fig. 9. Absorption spectra of dye C_5 in different solvents (10^{-4} M)

Table 3
Electronic absorption and fluorescence data of the synthesized azo dyes (C_1-C_5)

Solvents		C_1	C_2	C_3	C_4	C_5
DMSO	λ_{ex}	449	440	456	488	438
	Log ε	4.14	3.84	4.06	3.71	3.56
	λ_{em}	593	583	602	617	600
	ϕ	0.009	0.009	0.008	0.012	0.011
DMF	λ_{ex}	448	430	452	453	413
	Log ε	4.10	4.18	3.79	3.75	3.85
	λ_{em}	583	580	600	610	596
	ϕ	0.012	0.011	0.009	0.019	0.015
Ethanol	λ_{ex}	424	422	452	405	412
	Log ε	4.00	4.02	3.79	3.75	4.13
	λ_{em}	574	575	596	602	590
	ϕ	0.017	0.009	0.010	0.027	0.019
Toluene	λ_{ex}	410	421	445	423	407
	Log ε	3.91	4.08	3.03	3.64	3.79
	λ_{em}	568	570	593	602	588
	ϕ	0.021	0.016	0.020	0.032	0.028
n-Hexane	λ_{ex}	409	410	436	402	406
	Log ε	3.74	3.51	3.69	2.63	3.84
	λ_{em}	561	568	590	593	586
	ϕ	0.031	0.019	0.027	0.038	0.035

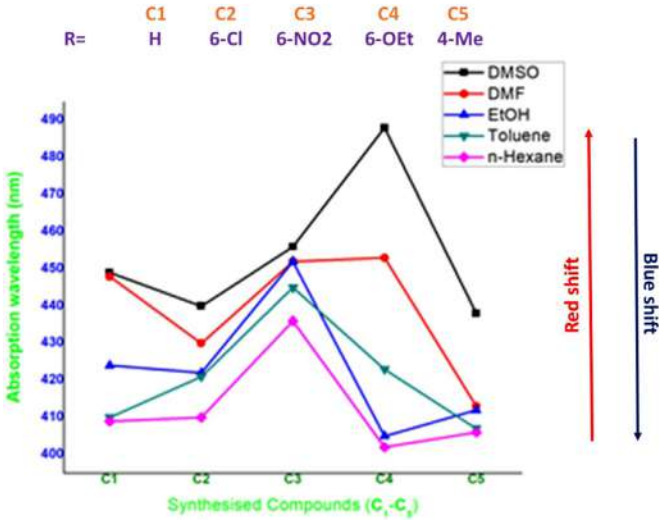

Fig. 10. Comparative graph of λ_{max} of dyes (C_1-C_5) in different solvents (10^{-4} M)

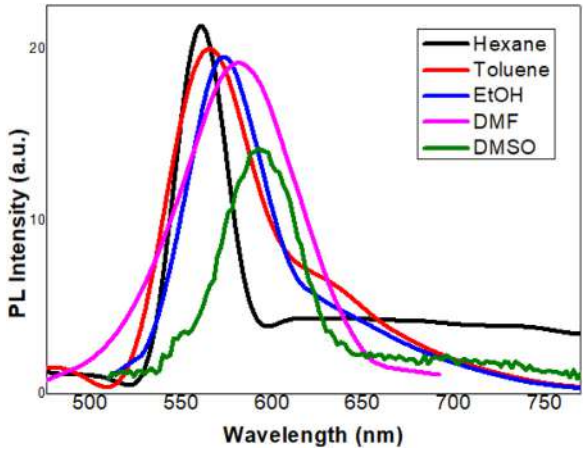

Fig. 11. Fluorescence spectra of dye C_1 in different solvents (10^{-4} M)

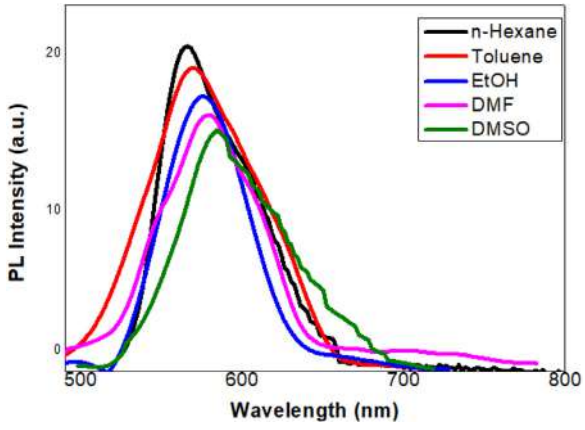

Fig. 12. Fluorescence spectra of dye C_2 in different solvents (10^{-4} M)

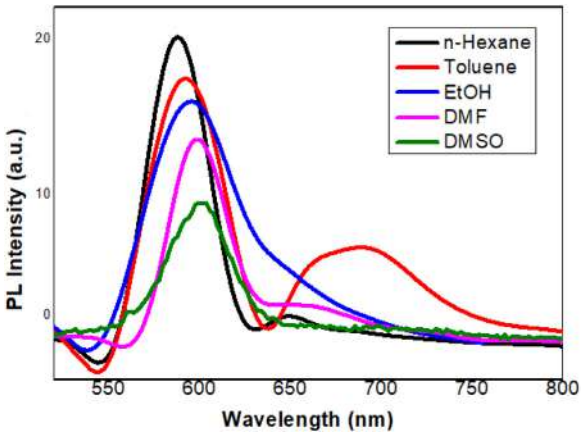

Fig. 13. Fluorescence spectra of dye C_3 in different solvents (10^{-4} M)

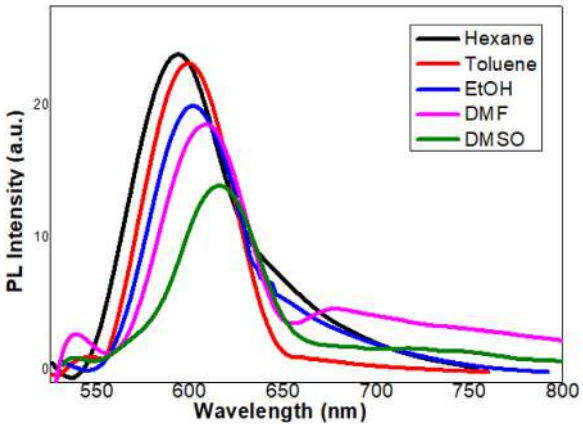

Fig. 14. Fluorescence spectra of dye C_4 in different solvents (10^{-4} M)

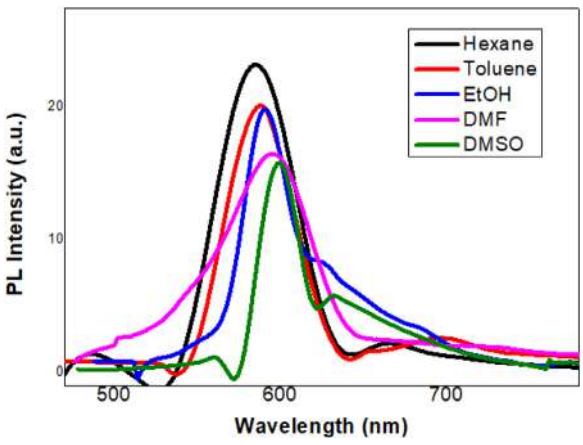

Fig. 15. Fluorescence spectra of dye C_5 in different solvents (10^{-4} M)

The quantum yield (QY) of the synthesized dye was calculated using the following formula [62] and values were appended in Table 3.

$$QY = QY_{ref}\frac{\eta^2}{\eta_{ref}^2}\frac{IA_{ref}}{AI_{ref}}$$

where, 'QY_{ref}' is the quantum yield of the reference (Rhodamine B, QY is 0.7 at room temperature) and 'I' is referred as the integrated fluorescence intensity or area under the curve. 'A' is the absorbance at the excitation wavelength, 'η' and 'η_{ref}' are the refractive indexes of test solvents and reference solvent respectively. The compounds C_4 and C_5 exhibited higher fluorescence intensity and quantum yield compared to other dyes, this is due to the presence of electron donating substituent such as –OEt and –Me at 6^{th} and 4^{th} position in compounds C_4 and C_5 respectively [63]. Compounds C_2 and C_3 displayed less fluorescence intensity and quantum yield among the synthesised dyes. This is attributed to presence of electron withdrawing groups such as –Cl and $-NO_2$ at 6^{th} position,

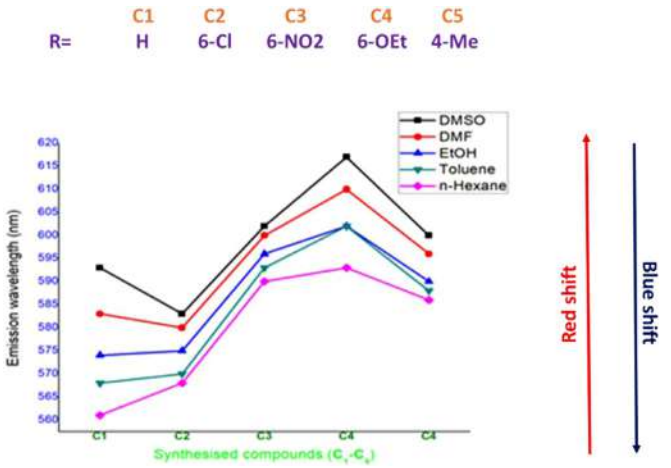

Fig. 16. Comparative graph of $\lambda_{emisson}$ of dyes (C_1-C_5) in different solvents (10^{-4} M)

which quenches the fluorescence intensity via inter-system crossing (ISC) or internal conversion (IC) [64].

3.4. Diffuse Reflectance (DR) spectral studies

To calculate the energy gap (Eg) of the synthesised dyes, DR spectra were recorded in the range of ~200–1000 nm at room temperature. Further, the energy gap (Eg) of the synthesised coumarin dyes (C_1-C_5) was calculated from the following Kubelka–Munk theory relations [65].

$$F(R) = \frac{(1 - R_\infty)}{2R_\infty} \quad (1)$$

$$h\nu = \frac{1240}{\lambda} \quad (2)$$

where R_∞ and λ are the reflection coefficient and absorption wavelength respectively. The DR spectra of dyes and plots of $[F(R_\infty)\ h\nu]^{1/2}$ versus photon energy (hv) were displayed in Fig. 17. The Eg value of the synthesised dyes (C_1-C_5) was found to be 2.71 eV, 2.51 eV, 2.73 eV, 2.52 eV, and 2.68 eV respectively which are well agreed with the calculated Eg values through DFT.

3.5. IR spectral data

IR spectra of the prepared dyes (C_1-C_5) were given in supplementary material (Fig. S6- S10). In the IR spectra, the –OH group stretching occurs in the range 3655-3752 cm^{-1}, the carbonyl of coumarin appeared in the range 1732-1746 cm^{-1}, -C=N displayed a stretching frequency in the region 1569-1656 cm^{-1} and a peak in the region 1482-1501 cm^{-1} corresponds to –N=N- functionality.

3.6. ^1H NMR and ^{13}C NMR spectral data

The structure of the synthesised compounds C_1-C_5 was authenticated by recording their ^1H NMR and ^{13}C NMR spectra in DMSO-*d6* solvent and obtained spectra were given in supplementary material (Fig. S11- S17). In ^1H NMR spectra, the aromatic protons resonated in the region 6.99-8.98 ppm as a multiplet. Additionally, compound C_4 showed a quartet at 3.98 ppm for $-CH_2-$ and as a triplet at 1.33 ppm for $-CH_3$ protons confirms the presence of $-OCH_2CH_3$ group. Similarly, C_5 displayed a singlet at 2.59 ppm for $-CH_3$ protons. However, the signals due to –OH protons attached to

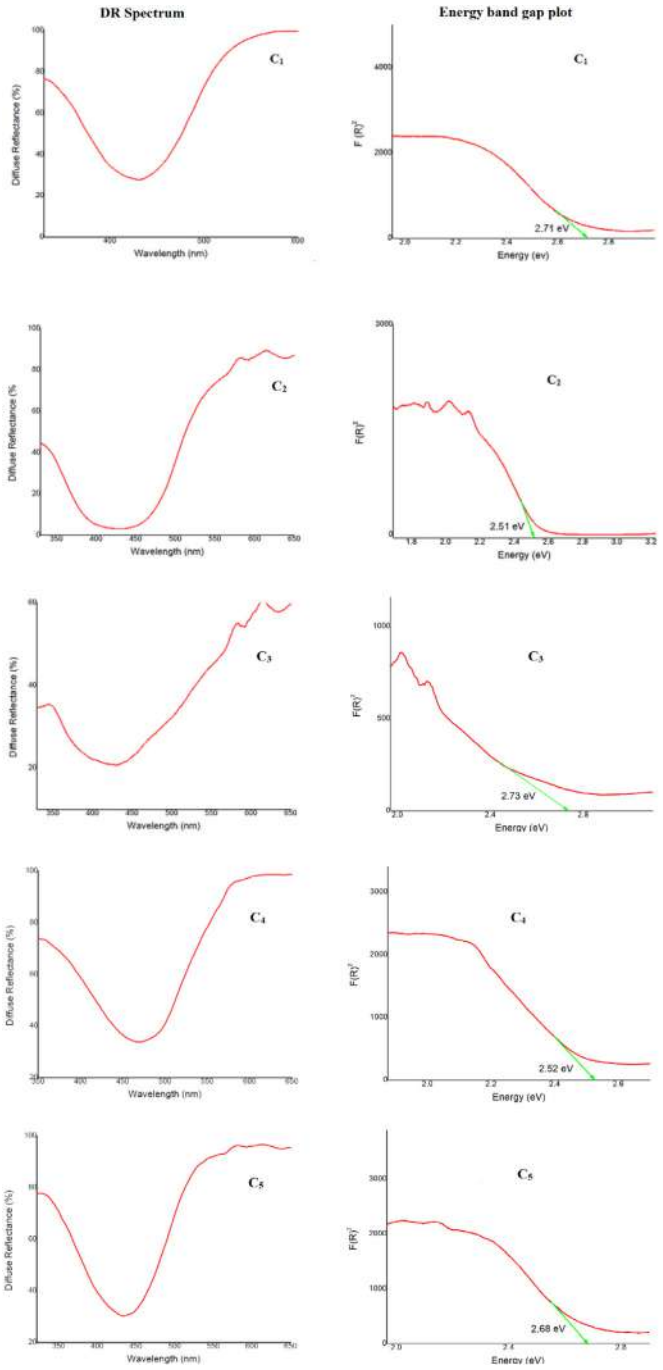

Fig. 17. DR spectrum and energy band gap plot of synthesised dyes (C_1-C_5)

the coumarin ring was not appeared in the NMR spectra, it may be due to interaction with DMSO-*d6* [66].

In ^{13}C NMR spectra, the compounds C_1 and C_2 displayed a peak due to lactone carbonyl carbon at 165.22 and 171.79 ppm respectively. Additionally, C-O carbon resonates at 157.57 and 157.52 ppm respectively. Other aromatic carbons of compounds C_1 and C_2 resonates in the range 117.87-154.54 ppm. But unfortunately, due to the poor solubility of compounds C_3-C_5 in DMSO, their ^{13}C spectra were not recorded.

3.7. Mass spectral data

The synthesized azo dyes (C_1-C_5) were studied for their HR-MS studies and the spectra were displayed in the supplemen-

Table 4
Antimycobacterial activity of synthesized coumarin dyes (C_1-C_5)

Sl. No.	Sample	100 µg/ml	50 µg/ml	25 µg/ml	12.5 µg/ml	6.25 µg/ml	3.12 µg/ml	1.6 µg/ml	0.8 µg/ml
01	C_1	S	S	S	S	S	S	S	R
02	C_2	S	S	S	S	S	S	S	R
03	C_3	S	S	S	S	S	S	S	R
04	C_4	S	S	S	S	S	R	R	R
05	C_5	S	S	S	S	S	S	S	R

NOTE: S- Sensitive; R- Resistant; Strain used: M. Tuberculosis (H_{37} RV strain): ATCC No- 27294. Here are the standard values for the Anti-TB test which was performed. Isoniazid- 1.6 µg/mL, Ethambutol- 3.2 µg/mL, Pyrazinamide - 3.125 µg/mL, Rifampicin- 0.8 µg/mL, Streptomycin- 0.8 µg/mL.

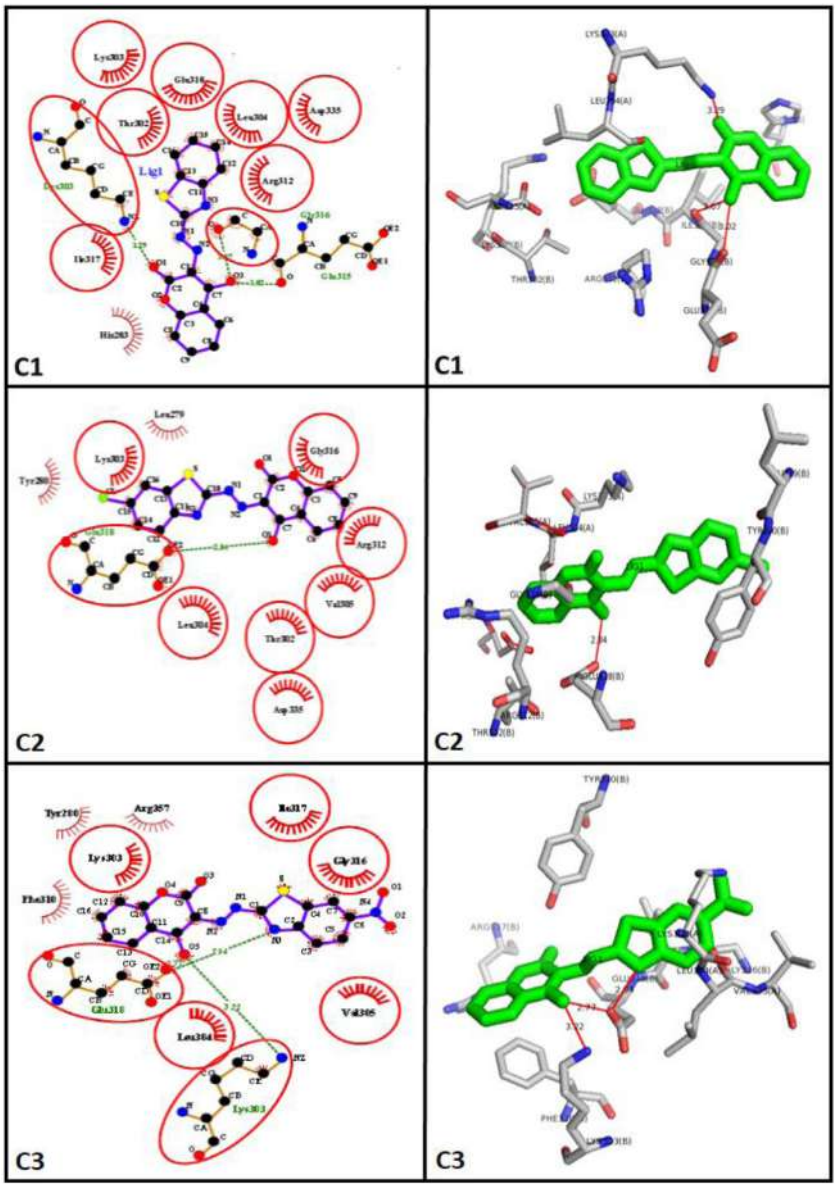

Fig. 18. 2D and 3D representation of the interaction of synthesised compounds (C_1-C_5) and Streptomycin with enoyl-ACP reductase (continued)

tary material (Fig. S18-S22). The HR-MS spectra of the compounds (C_1-C_5) exhibited molecular ion peaks due to $[M+H]^+$ at *m/z* 324.1071, 358.0699, 369.0903, 368.1315, and 338.1166 corresponding to their molecular weights 323.3259, 357.7710, 368.3235, 367.3785 and 337.3525 respectively. The obtained molecular ion peaks are precisely agreed with the molecular weight of the compounds.

3.8. Antimycobacterial activity

Tuberculosis is a deadly disease, mainly attacks the lungs and it transmits from person to person through the air [67]. The efficacy of the synthesised dyes (C_1-C_5) was checked against *Mycobacterium tuberculosis* (H37 RV strain) and compared the results with the standard drugs using microplate

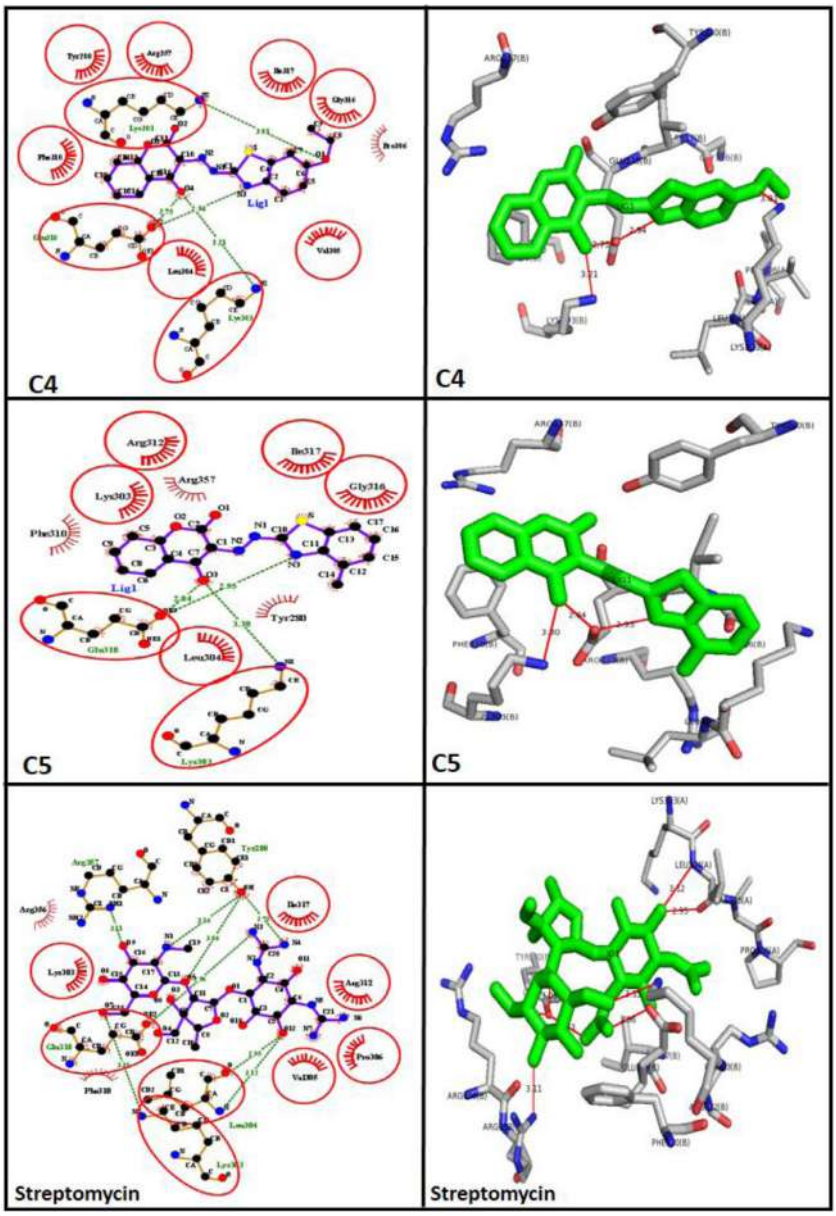

Fig. 18. Continued

Alamar Blue Assay (MABA) method. The results were tabulated in Table 4. The anti-TB activity results revealed that compounds C_1, C_2, C_3 and C_5 irrespective of their substitution exhibited excellent and similar sensitivity (MIC=1.6µg/mL) relative to standard streptomycin (MIC= 6.24 µg/mL). But the compound C_4 having ethoxy substitution at 6^{th}position of benzothiazole showed less sensitivity (MIC= 3.2µg/mL) among the synthesised dyes.

3.9. in silico *Molecular docking studies*

The enoyl-ACP reductase (InhA) in *Mycobacterium tuberculosis* is an attractive target for the development of novel drugs against tuberculosis. Inhibition of InhA blocks mycolic acid biosynthesis, thereby impairing the integrity of the cell wall and eventually leading to cell death [68].

Furthermore, analysis of interactions between the enoyl-ACP reductase and the ligands was carried out to identify the most significantly interacting residues and the type of thermodynamic interactions responsible for the binding of these molecules. 2D and 3D representations of the interaction of synthesised compounds (C_1-C_5) and streptomycin with enoyl-ACP reductase have been shown in Fig. 18 and the obtained results are appended in Table 5. From the results, it was observed that all the docked ligands C_1-C_5 showed excellent and almost similar binding energy in the range of -7.4 to -7.1 Kcal/mol compared to standard drug streptomycin (-6.1Kcal/mol). Compound C_4 form four hydrogen bonds: Among them, coumarin –OH form two H-bonds with amino acid residues Glu318 and Lys303 at a distance of 2.75 and 3.1A^0 respectively, nitrogen present in the benzothiazole ring form one H-bond with Glu318 residue at a distance of 2.94 A^0, and the oxygen of –OEt group form forth hydrogen bond with LYS303 at a distance of 3.01 A^0. Compound C_2 forms only one H-bond at a distance of 2.84A^0 with a residue Glu318, while the remaining compounds (C_1, C_3, C_5) individually form three H-bonds with amino acid residues. All the synthesised dyes displayed some appreciable hydrophobic interactions with the receptor.

Table 5
Displaying H-bonds, H-bond length, H-bond formation, Hydrophobic Interaction, Binding energy (kcal/mol) of the synthesized molecules(C_1-C_5) and Streptomycin after in silico docking

Compounds	Hydrogen Bonds	H-Bond Length (A^0)	H-Bond with	Hydrophobic interactions	Binding Energy (kcal/mol)
C_1	3	3.02 3.07 3.29	C1:O3:: Glu315:O C1:O3:: Gly316:O C1:O1::Lys303:NZ	His283, Ile317, Arg312, Glu318, Leu304, Thr302,Asp335,Lys303	-7.2
C_2	1	2.84	C2:O3::Glu318:OE2	Tyr280, Leu279, Lys303, Gly316, Val305, Leu304, Arg312,Asp335,Thr302	-7.1
C_3	3	2.77 2.94 3.22	C3:O5::Glu318:OE2 C3:N3::Glu318:OE2 C3:O5:: Lys303:NZ	Arg357, Phe310, Tyr280, Val305, Ile317, Lys303, Leu304,Gly316	-7.2
C_4	4	2.75 2.94 3.01 3.21	C4:O4::Glu318:OE2 C4:N3::Glu318:OE2 C4:O1::LYS303:NZ C4:O4::LYS303:NZ	Arg357, Phe310, Tyr280, Val305, Ile317, Pro306, Leu304,Gly316	-7.1
C_5	3	2.84 2.95 3.30	C5:O3::Glu318:OE2 C5:N3::Glu318:OE2 C5:O3::LYS303:NZ	Gly316, Lys303, Leu304, Ile317, Arg312,Tyr280, Arg357, Phe310	-7.4
Streptomycin	8	2.73 2.95 2.96 3.06 3.11 3.12 3.16 3.35	STR:N4::Tyr280:OH STR:O12::Leu304:O STR:N3::Glu318:OE2 STR:O5::Tyr280:OH STR:O9::Arg357:NH1 STR:O12::Leu304:N STR:N1::Tyr280:OH STR:O7::LYS303:NZ	Val305, Ile317, Pro306, Lys303, Phe310, Arg312, Arg356	-6.1

4. Conclusion

In the present study, we have synthesized the 4-hydroxy coumarin-benzothiazole based azo dyes by the diazo-coupling reaction of substituted 2-aminobenzothiazoles with 4-hydroxy coumarin at ice cold condition. The synthesised dyes were characterized by various analytical and spectroscopic techniques. The synthesised dyes exhibited a positive solvatochromic behaviour in absorption and emission study. Various properties of the dyes were studied by using DFT. Further, the synthesised azo dyes were screened for antituberculosis activity and *in silico* molecular docking studies. The results indicated that all the compounds showed promising activity and good docking scores compared to a standard drug.

Credit Authors statement

Manjunatha B: Methodology, Investigation, Writing - original draft. Yadav D. Bodke: Investigation, Supervision, Writing - review & editing. Nagaraja O: Writing - draft, Formal analysis. Lohith T. N: Formal analysis and Software, writing. Nagaraju G: Writing - review & editing. Sridhar M. A: Analysis and Software

Declaration of Competing Interest

With reference to the above subject, we hereby declare that the authors do not have any conflict of interest

Acknowledgements

The authors are thankful to the Chairman, Department of Chemistry, Kuvempu University, Shankaraghatta for providing the lab facilities and the University of Mysore for providing spectral data. One of the authors, Manjunatha B thankful to Council for Scientific and Industrial Research (CSIR), New Delhi, India, for the award of Junior Research fellowship [09/908(0011)/2019-EMR-I].

Supplementary materials

Supplementary material associated with this article can be found, in the online version, at doi;10.1016/j.molstruc.2021.131170.

References

[1] A. Panitsiri, S. Tongkhan, W. Radchatawedchakoon, U. Sakee, Synthesis and anion recognition studies of novel bis(4-hydroxycoumarin) methane azo dyes, J. Mol. Struct. 1107 (2016) 14–18, doi:10.1016/j.molstruc.2015.11.013.
[2] Y. Erdogdu, U.C. Baskose, S. Saglam, M. Erdogdu, H. Ogutcu, S. Özçelik, Structural, thermal, spectroscopic, electronic and biological activity properties of coumarin-153 dyes for DSSCs: A DFT benchmark study, J. Mol. Struct. 1221 (2020) 128873, doi:10.1016/j.molstruc.2020.128873.
[3] O. Nagaraja, Y.D. Bodke, R. Kenchappa, S.Ravi Kumar, Synthesis and characterization of 3-[3-(1H-benzimidazol-2-ylsulfanyl)-3-phenyl propanoyl]-2H-chromen-2-one derivatives as potential biological agents, Chem. Data Collect. 27 (2020) 100369, doi:10.1016/j.cdc.2020.100369.
[4] I.O. Akchurin, A.I. Yakhutina, A.Y. Bochkov, N.P. Solovjova, M.G. Medvedev, V.F. Traven, Novel push-pull fluorescent dyes–7-(diethylamino) furo-and thieno [3, 2-c] coumarins derivatives: structure, electronic spectra and TD-DFT study, J. Mol. Struct. 1160 (2018) 215–221, doi:10.1016/j.molstruc.2018.01.086.
[5] O. Nagaraja, Yadav D. Bodke, Itte Pushpavathi.S.Ravi Kumar, Synthesis, characterization and biological investigations of potentially bioactive heterocyclic compounds containing 4-hydroxy coumarin, Heliyon 6 (2020) e04245 4245-4255, doi:10.1016/j.heliyon.2020.e04245.
[6] G. Bakhtiari, S. Moradi, S. Soltanali, A novel method for the synthesis of coumarin laser dyes derived from 3-(1H-benzoimidazol-2-yl) coumarin-2-one under microwave irradiation, Arab. J. Chem. 7 (2014) 972–975, doi:10.1016/j.arabjc.2010.12.012.
[7] N. Obaiah, Y.D. Bodke, S. Telkar, Synthesis of 3-[(1H-Benzimidazol-2-ylsulfanyl)(aryl) methyl]-4-hydroxycoumarin Derivatives as Potent Bioactive Molecules, Chemistry Select 5 (2020) 178–184, doi:10.1002/slct.201903472.
[8] V. Venkatraman, S. Abburu, B.K. Alsberg, Artificial evolution of coumarin dyes for dye sensitized solar cells, Phys. Chem. Chem. Phys. 17 (2015) 27672–27682, doi:10.1039/C5CP04624F.
[9] K.V. Basavarajappa, Y. Arthoba Nayaka, H.T. Purushothama, R.O. Yathisha, M.M. Vinay, B.J. Rudresha, K.B. Manjunatha, Optical, electrochemical and current– voltage characteristics of novel coumarin based 2, 4-dinitrophenylhydrazone derivatives, J. Mol. Struct. 1199 (2020) 126946–126958, doi:10.1016/j.molstruc.2019.126946.
[10] M.D. Naik, Yadav D. Bodke, M Vijay Kumar, B.C. Revanasiddappa, An efficient one-pot synthesis of coumarin-amino acid derivatives as potential anti-inflammatory and antioxidant agents, Synth. Commun. 50 (2020) 1210–1216, doi:10.1080/00397911.2020.1735442.
[11] R.S. Keri, B.S. Sasidhar, B.M. Nagaraja, M.A. Santos, Recent progress in the drug development of coumarin derivatives as potent antituberculosis agents, Eur. J. Med. Chem. 100 (2015) 257–269, doi:10.1016/j.ejmech.2015.06.017.

[12] C.A. Kontogiorgis, D.J. Hadjipavlou-Litina, Synthesis and antiinflammatory activity of coumarin derivatives, J. Med. Chem. 48 (2005) 6400–6408, doi:10.1021/jm0580149.
[13] B.S. Kirkiacharian, E. De Clercq, R. Kurkjian, C. Pannecouque, New synthesis and anti-HIV and antiviral properties of 3-arylsulfonyl derivatives of 4-ydroxycoumarin and 4-hydroxyquinolone, Pharmaceut. Chem. J. 42 (2008) 265–270, doi:10.1007/s11094-008-0103-0.
[14] Y. Hu, Z. Xu, S. Zhang, X. Wu, J. Ding, Z. Lv, L. Feng, Recent developments of coumarin-containing derivatives and their anti-tubercular activity, Eur. J. Med. Chem. 136 (2017) 122–130, doi:10.1016/j.ejmech.2017.05.004.
[15] A. Bye, H.K. King, The biosynthesis of 4-hydroxycoumarin and dicoumarol by Aspergillus fumigatus Fresenius, Biochem. J. 117 (1970) 237–245, doi:10.1042/bj1170237.
[16] P.K. Jauhari, A. Bhavani, S. Varalwar, K. Singhal, P. Raj, Synthesis of some novel 2-substituted benzoxazoles as anticancer, antifungal, and antimicrobial agents, Med. Chem. Res. 17 (2008) 412–424, doi:10.1007/s00044-007-9076-x.
[17] A. Mohammadi, H. Ghafoori, B. Ghalami-Choobar, R. Rohinejad, Synthesis, solvatochromic properties and biological evaluation of some novel azo-hydrazone tautomeric dyes, J. Mol. Liq. 198 (2014) 44–50, doi:10.1016/j.molliq.2014.07.005.
[18] A. Alimmari, B. Bozic, D. Mijin, A. Marinkovic, N. Valentic, G. Uscumlic, Synthesis, structure and solvatochromic properties of some novel 5-arylazo-6-hydroxy-4-(4-methoxyphenyl)-3-cyano-2-pyridone dyes: hydrazone-azo tautomeric analysis, Arab. J. Chem. 2 (2015) 269–278, doi:10.1016/j.arabjc.2013.10.001.
[19] J.M.Cole Zhang, P.G. Waddell, K.S. Low, X. Liu, Relating electron donor and carboxylic acid anchoring substitution effects in azo dyes to dye-sensitized solar cell performance, ACS Sustain. Chem. Eng. 1 (2013) 1440–1452, doi:10.1021/sc400183t.
[20] A.S. Shawali, I.F. Zeid, M.H. Abdelkader, Alsayed A. Elsherbini, F.M.A. Altalbawy, Synthesis, Acidity Constants and Tautomeric Structure of 7-Arylhydrazono [1, 2, 4] Triazolo [3, 4-b][1, 3, 4] thiadiazines in Ground and Excited States, J. Chin. Chem. Soc 48 (2001) 65–72, doi:10.1002/jccs.200100012.
[21] J. Sahoo, S.K. Mekap, P.S. Kumar, Synthesis, spectral characterization of some new 3-heteroaryl azo 4-hydroxy coumarin derivatives and their antimicrobial evaluation, J. Taibah Univ. Sci. 9 (2015) 187–195, doi:10.1016/j.jtusci.2014.08.001.
[22] M.R. Yazdanbakhsh, A. Ghanadzadeh, E. Moradi, Synthesis of some new azo dyes derived from 4-hydroxy coumarin and spectrometric determination of their acidic dissociation constants, J. Mol. Liq. 136 (2007) 165–168, doi:10.1016/j.molliq.2007.03.005.
[23] M.A. Metwally, S. Bondock, E.I. El-Desouky, M.M. Abdou, Synthesis, structure elucidation and application of some new azo disperse dyes derived from 4-hydroxycoumarin for dyeing polyester fabrics, Am. J. Chem. 2 (2012) 347–354 https://doi.org/10. 5923/j.chemistry.20120206.09.
[24] B. Soni, M.S. Ranawat, R. Sharma, A. Bhandari, S. Sharma, Synthesis and evaluation of some new benzothiazole derivatives as potential antimicrobial agents, Eur. J. Med. Chem. 45 (2010) 2938–2942, doi:10.1016/j.ejmech.2010.03.019.
[25] N.Herrera Cano, M.S. Ballari, A.G. Lopez, A.N. Santiago, New synthesis and biological evaluation of benzothiazole derivates as antifungal agents, J. Agric. Food Chem. 63 (2015) 3681–3686, doi:10.1021/acs.jafc.5b00150.
[26] S.T. Huang, I.J. Hsei, C. Chen, Synthesis and anticancer evaluation of bis (benzimidazoles), bis (benzoxazoles), and benzothiazoles, Bioorg. Med. Chem 14 (2006) 6106–6119, doi:10.1016/j.bmc.2006.05.007.
[27] M. Singh, S.K. Singh, M. Gangwar, G. Nath, S.K. Singh, Design, synthesis and mode of action of some benzothiazole derivatives bearing an amide moiety as antibacterial agents, RSC Adv 4 (2014) 19013–19023, doi:10.1039/C4RA02649G.
[28] Jianjun Qi, C.H. Tung, Development of benzothiazole 'click-on'fluorogenic dyes, Bioorg. Med. Chem. Lett. 21 (2011) 320–323, doi:10.1016/j.bmcl.2010.11.009.
[29] K. Wen, X. Guo, J. Zhang, Computational prediction on photophysical properties of two excited state intramolecular proton transfer (ESIPT) fluorophores bearing the benzothiazole group, Mol. Phys. 117 (2019) 804–812, doi:10.1080/00268976.2018.1542169.
[30] F.U. Eze, U.C. Okoro, D.I. Ugwu, S.N. Okafor, Biological activity evaluation of some new benzenesulphonamide derivatives, Front. Chem. 7 (2019) 634–645, doi:10.3389/fchem.2019.00634.
[31] M.Sirous A.D.Khosravi, Z. Absalan, M.R. Tabandeh, M. Savari, Comparison of drrA and drrB efflux pump genes expression in drug-susceptible and-resistant Mycobacterium tuberculosis strains isolated from tuberculosis patients in Iran, Infect. Drug Resist. 12 (2019) 3437–3444, doi:10.2147/2/FIDR.S221823.
[32] V.T. Angelova, V. Valcheva, N.G. Vassilev, R. Buyukliev, G. Momekov, I. Dimitrov, B. Shivachev, Antimycobacterial activity of novel hydrazide-hydrazone derivatives with 2H-chromene and coumarin scaffold, Bioorg. Med. Chem. Lett. 27 (2017) 223–227, doi:10.1016/j.bmcl.2016.11.071.
[33] P.F. Dalberto, E.V. De Souza, B.L. Abbadi, C.E. Neves, R.S. Rambo, A.S. Ramos, L.A. Basso, The many hurdles on the way to anti-tuberculosis drug development, Front. Chem. 8 (2020) 1–27, doi:10.3389/fchem.2020.586294.
[34] J.N. Akester, P. Njaria, A. Nchinda, C.Le Manach, A. Myrick, V. Singh, K. Chibale, Synthesis, Structure–Activity Relationship, and Mechanistic Studies of Aminoquinazolinones Displaying Antimycobacterial Activity, ACS infectious diseases, 6 (2020) 1951–1964, doi:10.1021/acsinfecdis.0c00252.
[35] S. Govori, V. Kalaj, O. Leci, Synthesis and in vitro biological evaluation of 3, 4-annelated coumarin-pyrimido-pyrimidine systems, Toxicol. Environ. Chem. 96 (2014) 831–836, doi:10.1080/02772248.2014.974307.
[36] A. Sharma, S. Gudala, S.R. Ambati, S. Penta, Y. Bomma, V.R. Janapala, A. Kumar, Synthesis, Anticancer Evaluation, and Molecular Docking Studies of Novel (4-Hydroxy-2-Thioxo-3,4-Dihydro-2H-[1,3]Thiazin-6-Yl)-Chromen-2-Ones via a Multicomponent Approach, J. Chin. Chem. Soc. 65 (2018) 810–821, doi:10.1002/jccs.201700340.
[37] I.T. Bazyl, S.P. Kisil, Y.V. Burgart, V.I. Saloutin, Reactions of 4-hydroxy-5, 6, 7, 8-tetrafluorocoumarin derivatives with S-nucleophiles, J. Fluor. Chem. 103 (2000) 3–12, doi:10.1016/S0022-1139(99)00210-9.
[38] Y.V. Burgart, V.I. Saloutin, Derivatives of 4-hydroxy-5, 6, 7, 8-tetrafluorocoumarin in reactions with o-aminothiophenol, Russ. J. Electrochem. 36 (2000) 904–909.
[39] M.M. Makhlouf, H.M. Zeyada, Synthesis, structural analysis, spectrophotometric measurements and semiconducting properties of 3-phenyl azo-4-hydroxycoumarin thin films, Synth. Met. 211 (2016) 1–13, doi:10.1016/j.synthmet.2015.10.019.
[40] M.R. Shreykar, A. Jadhav, N. Sekar, Aggregation induced emissive and NLOphoric coumarin thiazole hybrid dyes: Synthesis, photophysics and TD-DFT studies, J. Lumin. 188 (2017) 38–53, doi:10.1016/j.jlumin.2017.03.053.
[41] A. Bhattacharyya, N. Guchhait, Proton transfer inhibited charge transfer in a coumarinyl chalcone: Hassle free detection of chloroform vapor in alcohol medium and in neat solution, Spectrochim. Acta A Mol. Biomol. Spectrosc. 253 (2021) 119578, doi:10.1016/j.saa.2021.119578.
[42] D. Zhou, D. Ma, Y. Wang, X. Liu, X. Bao, Study with density functional theory method on methane C–H bond activation on the MoO2/HZSM-5 active center, Chem. Phys. Lett 2 (2003) 46–51, doi:10.1016/S0009-2614(03)00513-X.
[43] J. Leconte, A. Markovits, M.K. Skalli, C. Minot, A. Belmajdoub, Periodic ab initio study of the hydrogenated rutile TiO2 (1 1 0) surface, Surf. Sci. 1 (2002) 194–204, doi:10.1016/S0039-6028(01)01477-7.
[44] W. Kohn, A.D. Becke, R.G. Parr, Density functional theory of electronic structure, J. Phys. Chem. 100 (1996) 12974–12980, doi:10.1021/jp960669l.
[45] P. Hohenberg, W. Kohn, Inhomogeneous electron gas, Phys. Rev. 3 (1964) 864–871, doi:10.1103/PhysRev.136.B864.
[46] M.J.E.A Frisch, G.W. Trucks, H.B. Schlegel, G.E. Scuseria, M.A. Robb, J.R. Cheeseman, H. Nakatsuji, gaussian, Gaussian. Inc. 201 (2009) 09 Wallingford CT.
[47] H.B. Schlegel, Optimization of equilibrium geometries and transition structures, J. Comput. Chem. 3 (1982) 214–218, doi:10.1002/jcc.540030212.
[48] R. Ditchfield, D.P. Miller, J.A. Pople, Self-consistent molecular orbital methods. xi. molecular orbital theory of nmr chemical shifts, J. Chem. Phys. 10 (1971) 4186–4193, doi:10.1063/1.1674657.
[49] R. Dennington, T. Keith, J. Millam, GaussView, version 5, 2009.
[50] T. Lu, F. Chen, Monomeric adenine decay dynamics influenced by the DNA environment, J. Comput. Chem. 33 (2012) 580–592, doi:10.1002/jcc.22952.
[51] W. Humphrey, A. Dalke, K. Schulten, VMD: visual molecular dynamics, J. Mol. Graph. (1996) 33–38, doi:10.1016/0263-7855(96)00018-5.
[52] N.M. Mallikarjuna, J. Keshavayya, B.N. Ravi, Synthesis, spectroscopic characterization, antimicrobial, antitubercular and DNA cleavage studies of 2-(1H-indol-3-yldiazenyl)-4, 5, 6, 7-tetrahydro-1, 3-benzothiazole and its metal complexes, J. Mol. Str. 1173 (2018) 557–566, doi:10.1016/j.molstruc.2018.07.007.
[53] A.W. Schüttelkopf, D.M. Van Aalten, PRODRG: a tool for high-throughput crystallography of protein–ligand complexes, Acta Crystallogr. Sect. D: Biol. Crystallogr. 60 (2004) 1355–1363, doi:10.1107/S0907444904011679.
[54] S.R. Luckner, N. Liu, C.W. Am Ende, P.J. Tonge, C. Kisker, A slow, tight binding inhibitor of InhA, the enoyl-acyl carrier protein reductase from Mycobacterium tuberculosis, J. Biol. Chem. 285 (2010) 14330–14337, doi:10.1074/jbc.M109.090373.
[55] S. Dallakyan, A.J. Olson, Small-molecule library screening by docking with PyRx, Chemical biology. 41 (2015) 243-250 https://doi.org/10.1007/978-1-4939-2269-7_19.
[56] G. Gece, The use of quantum chemical methods in corrosion inhibitor studies, Corros. Sci. 50 (2008) 2981–2992, doi:10.1016/j.corsci.2008.08.043.
[57] D.F.V. Lewis, C. Ioannides, D.V. Parke, Interaction of a series of nitriles with the alcohol-inducible isoform of P450: Computer analysis of structure—activity relationships, Xenobiotica 24 (1994) 401–408, doi:10.3109/00498259409043243.
[58] D.V. Geetha, H.A. Fares, H.E.M. Yasseir, M.A. Sridhar, A.K. Shaukath, N.K. Lokanath, Design-based synthesis, molecular docking analysis of an anti-inflammatory drug, and geometrical optimization and interaction energy studies of an indole acetamide derivative, J. Mol. Str 1178 (2019) 384–393, doi:10.1016/j.molstruc.2019.127244.
[59] I. Fleming, Molecular orbitals and organic chemical reactions, John Wiley & Sons, 1977.
[60] T. Lu, F. Chen, Monomeric adenine decay dynamics influenced by the DNA environment, J. Comput. Chem. 33 (2012) 580–592, doi:10.1002/jcc.22952.
[61] E.R. Johnson, S. Keinan, P. Mori-Sánchez, J. Contreras-García, A.J. Cohen, W. Yang, Revealing noncovalent interactions, J. Am. Chem. Soc. 132 (2010) 6498–6506, doi:10.1021/ja100936w.
[62] T.C. Werner, W. Hawkins, J. Facci, R. Torrisi, T. Trembath, Substituent effects on the fluorescence properties of aromatic esters of 9-anthroic acid, J. Phys. Chem. 82 (1978) 298–301.
[63] S. Eskikanbur, K. Sayin, M. Kose, H. Zengin, V. McKee, M. Kurtoglu, Synthesis of two new azo-azomethines; spectral characterization, crystal structures, computational and fluorescence studies, J. Mol. Str. 1094 (2015) 183–194, doi:10.1016/j.molstruc.2015.03.043.
[64] Y.M. Poronik, G.V. Baryshnikov, I. Deperasińska, E.M. Espinoza, J.A. Clark, H. Agren, V.I. Vullev, Deciphering the unusual fluorescence in weakly coupled bis-nitro-pyrrolo [3, 2-b] pyrroles, Commun. Chem. 3 (2020) 1–18, doi:10.6086/D13X22.
[65] N. Kumar, K.M. Mahadevan, G. Nagaraju, Development and detection of level II and III features of latent fingerprints using highly sensitive AIE based coumarin

fluorescent derivative, J. Sci. Adv mater dev. 5 (2020) 520–526, doi:10.1016/j.jsamd.2020.09.004.
[66] B.N. Ravi, J. Keshavayya, N.M. Mallikarjuna, H.M Santhosh, Synthesis, characterization, cyclic voltammetric and cytotoxic studies of azo dyes containing thiazole moiety, Chem. Data Collect. 25 (2020) 100334, doi:10.1016/j.cdc.2019.100334.
[67] J.C. Palomino, A. Martin, Drug resistance mechanisms in Mycobacterium tuberculosis, Antibiotics 3 (2014) 317–340, doi:10.3390/antibiotics3030317.
[68] A.A. Upare, P.K. Gadekar, H. Sivaramakrishnan, N. Naik, V.M. Khedkar, D. Sarkar, S.M. Roopan, Design, synthesis and biological evaluation of (E)-5-styryl-1, 2, 4-oxadiazoles as anti-tubercular agents, Bioorg. Chem. 86 (2019) 507–512, doi:10.1016/j.bioorg.2019.01.054.